Optimization of Composite Wind Turbine Blade Based on Modal Sensitivity

ZHENG Yuqiao, LIU Zheyan, MA Huidong, ZHU Kai*

School of Mechanical and Electronical Engineering, Lanzhou University of Technology, Lanzhou 730050, P. R. China

(Received 10 June 2020; revised 20 July 2020; accepted 1 September 2020)

Abstract: This study develops a method for the full-size structural design of blade, involving the optimal layer thickness configuration of the blade to maximize its bending stiffness using a genetic algorithm. Numerical differentiation is employed to solve the sensitivity of blade modal frequency to the layer thickness of each part of blade. The natural frequencies of first-order flapwise and edgewise modes are selected as the optimal objectives. Based on the modal sensitivity analysis of all design variables, the effect of discretized layer thickness on bending stiffness of the blade is explored, and 14 significant design variables are filtered to drive the structural optimization. The best solution predicts an increase in natural frequencies of first-order flapwise and edgewise blade modes by up to 12% and 10.4%, respectively. The results show that the structural optimization method based on modal sensitivity is more effective to improve the structural performance.

Key words: composite blade; discrete layer thickness; modal sensitivity; optimal thickness distribution; bending stiffness

CLC number: TK83 **Document code:** A **Article ID:** 1005-1120(2021)01-0153-11

0 Introduction

The large horizontal-axis wind turbine blade, one of the most critical components of the wind power system, is characterized by slender shape, varying composite materials configurations, including sandwich construction[1-2]. Besides, blades are subjected to aerodynamic loading while working, which further increase the challenge of maintaining a safe distance between blades and tower[3]. Either glass-fiber or car-bon-fiber-reinforced polymers, or even hybrids of both fibers is utilized as the primary load-bearing materials[4-5]. Its long span, limited capacity to control blades tip deflection for ensuring a safe distance between blades tip and tower, along with the trend of individual wind turbine capacity increasing year by year, all suggest that it requires the higher bending stiffness than other small and medium blades[6]. For these horizontal-axis wind turbines (HAWTs), studies have found that the blade weight grows with a rotor radius at $R^{2.3}$ while the rotor power grows with $R^{2.1}$[7]. To ensure a safe distance between the blade and the tower, the blade stiffness must increase at least in proportion to its weight as the rotor radius grows. In addition to improvements in the blade bending stiffness in the design and manufacture process, structural optimization can be a practical approach to increase it[8-9].

Most of the published literature have described some specific issues of the structural optimization of the composite blades. Barr and Jaworski[10] explored the concept of passive aero elastic tailoring to maximize the power extraction of National Renewable Energy Laboratory (NREL) 5 MW wind turbine blade and presented a variable-angle tow composite materials model along blade span to couple the bend-twist deformations under aerodynamic load. The resulting computational formulation predicted an increase of 14% in turbine power extraction when the optimization is performed around the cut-in wind

*Corresponding author, E-mail address: mahuidonglut@163.com.

How to cite this article: ZHENG Yuqiao, LIU Zheyan, MA Huidong, et al. Optimization of composite wind turbine blade based on modal sensitivity[J]. Transactions of Nanjing University of Aeronautics and Astronautics, 2021, 38(1): 153-163.

http://dx.doi.org/10.16356/j.1005-1120.2021.01.015

speed, and by 7% when the blade is optimized near the rated wind speed. In Ref.[11], a high-fidelity multi-disciplinary optimization capability is employed for the structural optimization of wind turbine blades. The optimal fiber angles distribution through-out the internal structure of the blade were sought to minimize a stress parameter for each of several load cases. The result showed that the driving stress for fatigue has a reduction of 18%—60% after optimization. Almeida et al.[12] presented a methodology to perform cross-section evolutionary optimization for a topologically-optimized structure using a genetic algorithm. The structure with both topology and cross-section optimization accomplished a specific stiffness 330% higher than the structure of the quasi-isotropic stacking sequence. Buckney et al.[13] utilized the topology optimization to find optimal structural configurations for a 3 MW wind turbine blade and saved weight by up to 13.8% compared to a conventional design. There are two different approaches to achieve structural optimization of the blade. The first approach is the optimization in spanwise material distribution, the selection of materials, size of parts such as spar flange and shear webs through the knowledge of typical blade build-up and constraint, e.g. Refs.[10-11]. The other is topology optimization, which seeks the optimal material distribution, e.g. Refs.[12-13]. Here, the first approach will be applied to the structural optimization of the blade.

The researchers considered the size of blade parts as continuous design variables in the optimization problems. Chen et al.[14] developed a procedure to optimize composite structures of the wind turbine blades, which not only allows thickness variation but also considers it as a continuous variable. The results showed that the optimal mass of the blade is reduced significantly compared to the initial blade. Bottasso et al.[15] presented a similar parameterization method but with the addition of leading edge reinforcement and skin core, and this method resulted in 53 continuous thickness design variables. Two loops achieved the optimization. The inner loop used a 2-D cross-section finite element model by which the gradient-based optimization was finished. The criteria utilized in the inner loop was calibrated in turn by a finer 3-D finite element model used in the outer loop.

A discrete sizing of plies is achieved by formulating the optimization problems. Sjolund and Lund[16] minimized the mass of wind turbine blade while considering manufacturing constraints, tip displacement, buckling, and static strength criteria. Researches divided the blade into patches and selected the layer thicknesses as design variables, which were assumed discrete in the optimization. This gradient-based sizing optimization resulted in a reduction in mass and many practical constraints across multiple load directions. Fagan et al.[17] performed experimental testing on a 13 m long composite wind turbine blade and a design optimization to minimize the material used in blade construction by considering the discrete thickness distribution of the composite materials. While ample investigation is available to demonstrate that discrete layer size can be determined as design variables to drive structural optimization, the effect of discretized layer size on dynamic blade characteristics from a full-size perspective is still a challenging task.

To address this knowledge gap, first of all, the five main components of the blade, including the leading edge, leading edge panel, spar flange, trailing edge panel, and trailing edge, are equally divided into 27 segments along the blade span. The layup thickness of each patch, coupled with blade root and its transition, are considered as design variables, and natural frequencies of the first-order flapwise and edgewise modes are determined as the optimal objectives of this work. Final 14 design variables are selected by the modal sensitivity analysis of all design variables, and this optimization problem is solved using a genetic algorithm.

1 Methods and Models

1.1 Blade geometry

A 40.5 m blade design from a 1.5 MW turbine has been selected to conduct flapwise and edgewise bend stiffness optimum, and its tip displacement varies linearly with its bend stiffness. For this rea-

son, the bending stiffness of a long blade must maintain a safe distance between the blade tip and the tower under complex aerodynamic loads. The corresponding design parameters of the blade are listed in Table 1[18]. The aerodynamic airfoil surfaces of the blade are shown in Fig.1.

Table 1 Design parameter description[18]

Parameter	Value
Total length/m	40.5
Maximum chord length/m	3.184
Maximum twist angle/(°)	16
Blade root outer diameter/m	1.89
Position of maximum chord length/m	8

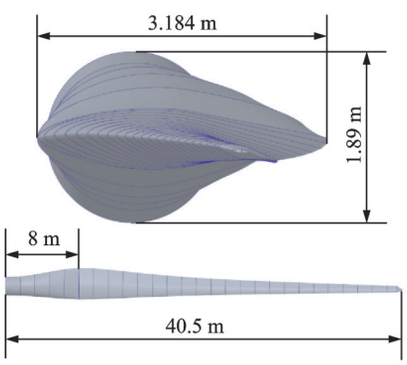

Fig.1 Blade geometry surface model

1.2 Blade structure

The structural model of the blade, including the construction of the composite structure, was created in ANSYS, a commercial finite element analysis code[19]. For a finite element analysis process, one of the most essential steps in executing the finite element analysis code is the creation of a structural finite element grid, and this blade structural grid has a total of 27 549 elements.

The design of the blade layup is to determine the angle and number of each layup angle according to the performance requirements and load characteristics of different parts of the blade. This process is decisive for the blade weight, performance and life. So it needs repeated iteration and continuous improvement. Glass fiber reinforced composite material is selected as the primary laminated material of the blade; other auxiliary materials include Balsa wood, polyvinyl chloride (PVC) foam, and reinforcement material[20]. The mechanical properties of these materials applied to the optimization of this work are listed in Table 2.

Table 2 Blade material properties

Material	E_x / GPa	E_y / GPa	G_{xy}/ GPa	υ	ρ/ (kg·m^{-3})
E-Glass UD	33.19	11.12	3.69	0.3	2 000
Balsa	2.07	2.07	0.106	0.02	80
PVC	0.087	0.087	0.031	0.45	80
Reinforcement	3.5	3.5	1.4	0.3	1 100
Resin epoxy	3.78	3.78	1.4	0.35	1 160

In Table 2, E_x and E_y are the Young's modulus in two principle directions, respectively, G_{xy} is the in-plane shear modulus, υ denotes Poisson' ratio, and ρ represents the material density. The wind turbine blade is a typical composite material structure. Its manufacture can be divided into five stages: materials, fabrics, stackups, sub laminates, blade. Materials: This stage is mainly to prepare the basic composition materials of the blade in Table 2. Fabrics: This stage aims to produce a single layer of fabric corresponding to each material in the first stage. The mechanical properties of each single-layer fabric are shown in Fig.2. Stackups: The lamination of single-layer fabrics forms the basic structure of blade manufacturing, such as uniaxial glass, biaxial glass, etc. Sub laminates: This stage aims to complete the layup of each sub-region of the blade according to the blade layup scheme. Blade: The overall composite structure of the blade is obtained by combining the sub-laminates of the fourth stage. It can be seen that the mechanical properties of the blade depend on the mechanical properties of the materials in Table 2 and the layup scheme of the blade. Therefore, these material properties play role through the layup scheme of the blade.

According to the layup materials in Table 2, uniaxial fabrics, biaxial fabrics, triaxial fabrics, balsa fabrics, PVC fabrics, and reinforcing material fabrics were manufactured. Corresponding mechanical properties of these fabrics were calculated and illustrated in Fig.2.

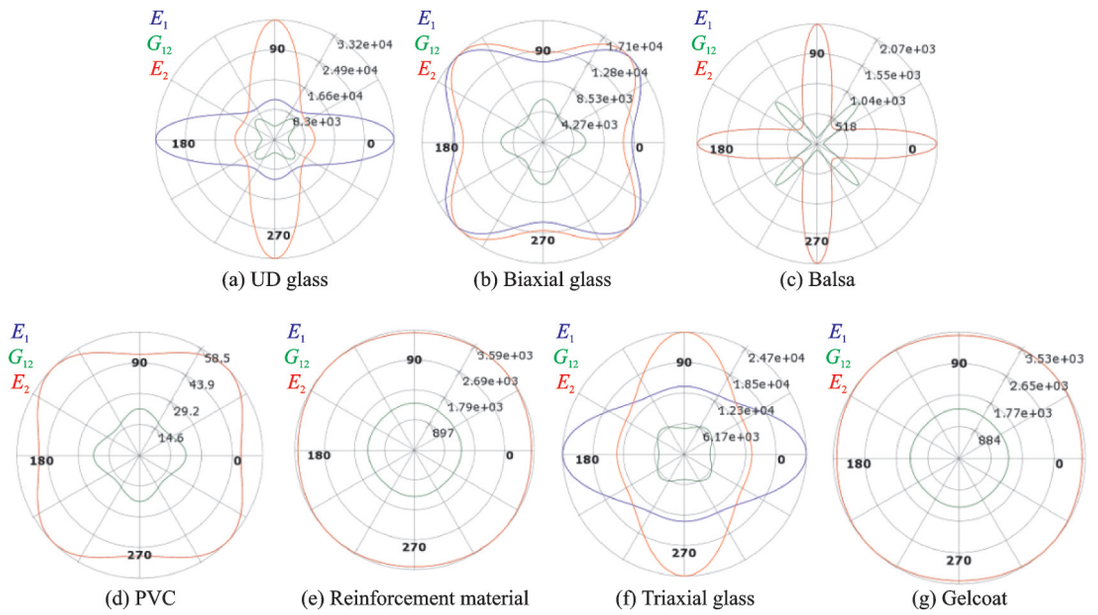

(a) UD glass (b) Biaxial glass (c) Balsa

(d) PVC (e) Reinforcement material (f) Triaxial glass (g) Gelcoat

Fig.2 Mechanical properties of single-layer fabrics

Fig.2 indicates elastic modulus is the largest among all single-layer fabrics, which is 33.2 GPa, and its shear modulus has a maximum value of 8.3 GPa in the ± 45° directions. The biaxial fabric has the largest elastic modulus in the directions of ± 45°, reaching 17.1 GPa, while the maximum value of the shear modulus occurs at the main directions of 0° and 90°. It is evident that the anisotropy of the biaxial fabric is not as significant as the uniaxial fabric. For Balsa single-layer fabric, its elastic modulus is much lower than that of uniaxial and biaxial fabrics, and there is only a second principal elastic modulus with a maximum value of 2.07 GPa. Its shear modulus has a maximum value of 1.04 GPa in the ± 45° directions. PVC single-layer fabric is almost an isotropic material, its elastic modulus and shear modulus are the lowest among all single-layer fabrics, and the corresponding maximum values are 58.5 MPa and 21.9 MPa, respectively. Reinforcement and Gelcoat single-layer fabrics are two isotropic materials in all single-layer fabrics and have similar mechanical properties.

The blade root consists of the 0.6 mm-thick triaxial fabric, and its total thickness reaches 96.6 mm. The spar flange is laid by the 0.97 mm-thick uniaxial fabric with two layers of 0.6 mm-thick Gelcoat fabrics on the outside of the blade. The large stack-ups of uniaxial fabric on the spar flange to increase the bending stiffness so that the tip displacements of the designed blade have a similar amplitude to those operated in real conditions. The shear webs are laminated from a 30 mm-thick core material (PVC) with two layers of ±45° glass fiber (0.57 mm-thick biaxial fabric) on one side and two layers of ±45° glass fiber on the other side. The lamination on the shear webs greatly enhances the shear resistance of the blade, and the effect of bend-twist coupling. The trailing edge panel has a similar construction as the shear webs, but the core material PVC is replaced with the 20 mm-thick Balsa wood. The entire inner surface of the blade is laid with two layers of 1.2 mm-thick reinforcement material, and the blade skin is made of two layers of 0.6 mm-thick Gelcoat, which generates a smooth aerodynamic surface of the blade. Because the layup of the blade is carried out in sections and regions, there will be many areas of abrupt thickness drop between any two sections. For these areas, the epoxy resin is applied to fill for reducing local stress concentration. The direction from the root to the tip of the blade as a 0° of ply orientation and fiber angles are defined as unfavorable if they are biased towards the leading edge for 0° direction of ply orientation. The leading and trailing edges of the blade mainly consists of uniaxial fabric and reinforcing material.

1.3 Modal analysis and natural frequencies

From the perspective of vibration analysis and control of a structure, any vibration system can be uniformly characterized by the source-path-receiver model, as shown in Fig.3.

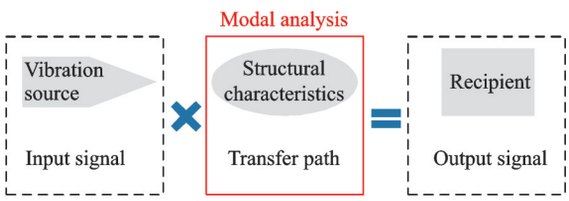

Fig.3 Source-path-receiver model

Fig.3 displays that the modal analysis mainly explores the second part of the model, namely the structural vibration characteristics, to obtain the natural vibration characteristics such as the modal parameters of the structure. The modal parameters of the blade mainly consist of natural frequencies, mode shape, and damping coefficient, among which the natural frequency and damping coefficient are global characteristics, and the mode shape presents local characteristics. Because the investigation mainly focuses on improving the bending stiffness of the blade by varying the layer thickness of the blade, the characteristics of the natural blade frequency are highlighted.

According to the calculation formula of the natural frequency of the structure $f=\frac{1}{2\pi}\sqrt{\frac{\boldsymbol{K}}{\boldsymbol{M}}}$ ($\boldsymbol{K}$ is the structural stiffness matrix and $\boldsymbol{M}$ the structural mass matrix), when the structural weight remains unchanged, its natural frequency grows as the structural stiffness increases. In order to improve the flapwise and edgewise stiffness of the blade, the first two natural frequencies of the blade will be selected as the optimal objective. Using both Block Lanczos (BL) and test method to determine the modal parameters of the blade, and the first two orders' natural frequencies of the blade are extracted, as shown in Table 3. This table contains the calculated and tested modal parameters of the blade. The calculated modal parameters are solved by commercial finite element software ANSYS. The tested modal parameters are provided by companies that have a cooperative relationship with authors.

Table 3 First two orders natural frequencies of the blade

Modal order	BL /Hz	Test /Hz	Mode shape
1	0.75	0.76	Flapwise
2	1.16	1.17	Edgewise

1.4 Modal sensitivity

Modal frequency sensitivity is defined as the rate of change of the structure's natural vibration frequency with the structure parameters. The differential equation of undamped free vibration of a structure can be expressed as

$$(\boldsymbol{K}-\lambda_i\boldsymbol{M})\boldsymbol{f}_i=0 \tag{1}$$

where λ_i represents the ith eigenvalue, and f_i the ith natural frequency of the structure.

Assuming the jth design variable is x_j, the differential of Eq.(1) to x_j can be stated by Eq.(2)

$$(\boldsymbol{K}-\lambda_i\boldsymbol{M})\frac{\partial\boldsymbol{f}_i}{\partial x_j}+\left(\frac{\partial\boldsymbol{K}}{\partial x_j}-\lambda_i\frac{\partial\boldsymbol{M}}{\partial x_j}\right)\boldsymbol{f}_i=\frac{\partial\lambda_i}{\partial x_j}\boldsymbol{M}\varphi_i \tag{2}$$

Multiply $\boldsymbol{f}_i^{\mathrm{T}}$ on the left side of Eq.(2) and combine Eq.(1). The result can be formulated by Eq.(3)

$$\boldsymbol{f}_i^{\mathrm{T}}(\boldsymbol{K}-\lambda_i\boldsymbol{M})\frac{\partial\boldsymbol{f}_i}{\partial x_j}=0 \tag{3}$$

Therefore, the eigenvalue sensitivity of equation can be calculated as

$$\frac{\partial\lambda_i}{\partial x_j}=\frac{\boldsymbol{f}_i^{\mathrm{T}}\left(\frac{\partial\boldsymbol{K}}{\partial x_j}-\lambda_i\frac{\partial\boldsymbol{M}}{\partial x_j}\right)\boldsymbol{f}_i}{\boldsymbol{f}_i^{\mathrm{T}}\boldsymbol{M}\boldsymbol{f}_i} \tag{4}$$

where $\frac{\partial\boldsymbol{K}}{\partial x_j}$ is the first derivative of the structural stiffness matrix to x_j, and $\frac{\partial\boldsymbol{M}}{\partial x_j}$ the first derivative of the structural mass matrix to x_j.

In the present work, the differential approach with the advantage of relatively high calculation accuracy and low solution cost was employed to calculate the sensitivity of stiffness and mass matrices along the blade. The frequency sensitivity of the structural vibration equation can be obtained by

$$\frac{\partial\boldsymbol{f}_i}{\partial x_j}=\frac{1}{2\pi}\frac{\partial\lambda_i}{\partial x_j} \tag{5}$$

2 Parameter Optimization

2.1 Design variables

The natural frequencies of the blade are proportional to the stiffness of the blade when the blade's weight is constant. Here, the aim of bending stiffness optimization of the blade can be achieved by maximizing the natural frequencies of the blade, affected by the composite layup thickness in the spar flanges, leading and trailing edge, and leading and trailing panel. These parts are equally divided into 27 segments along the blade span, and the layup thickness of each point was considered a design variable for the bending stiffness optimization. A cubic spline interpolation was carried out between the points where the layup thickness is explicitly defined to obtain the layup thickness at any area along the blade span. The blade layup thickness is symmetrical about the spar flange to reduce computational costs and the complexity of blade layup operations. In other words, the design variables at the leading and trailing edges of the blade are equal in magnitude, and so are the design variables at the leading and trailing panels, as shown in Fig.4.

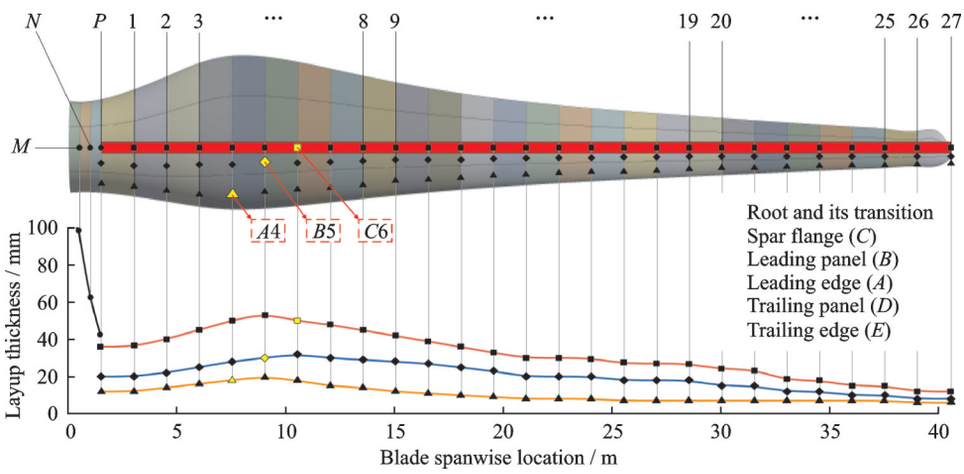

Fig.4 Symbolic representation of the design variables

Fig.4 illustrates the symbolic representation of the design variables. Blade root and its two transition positions are denoted by capital letters M, N and P. Leading edge, leading panel, spar flange, trailing panel, and trailing edge are represented by capital letters A, B, C, D, and E, respectively. This simple representation, which is exclusive for each design variable, is a combination of letters and numbers. For example, the three design variables highlighted in yellow in Fig.4 can be expressed as $A4$, $B5$ and $C6$.

2.2 Optimization model

The bending stiffness of the blade mainly includes the flapwise bending stiff-ness along the axial of the blade rotor and the edgewise bending stiffness in the rotation direction of the blade rotor, and the corresponding natural modes of these two bending stiffnesses are also significantly different. To create a positive correlation between natural frequencies and bending stiffness of the blade, the two optimization strategies are proposed. The first strategy determines the blade weight as a constraint to ensure the blade weight does not exceed the existing blade weight and the other strategy regards the blade weight as an optimization goal. The optimization problems are formally stated as

$$\begin{aligned} &\max f_1, f_2 \\ &\text{s.t. } m \leqslant m_0 \\ &x_{il} < x_i < x_{iu} \quad i=1,2,\cdots,14 \end{aligned} \tag{6}$$

$$\begin{aligned} &\max f_1, f_2, m \\ &x_{il} < x_i < x_{iu} \quad i=1,2,\cdots,14 \end{aligned} \tag{7}$$

where f_1 is the first-order flapwise natural frequency, f_2 the first-order edgewise natural frequency, m the blade weight, m_0 the existing blade weight, and x_i the design variables. x_{il} and x_{iu} are the lower and

upper limits of the design variables in the optimization problems.

Fig.5 shows the steps that these four schemes are performed in the optimization procedure.

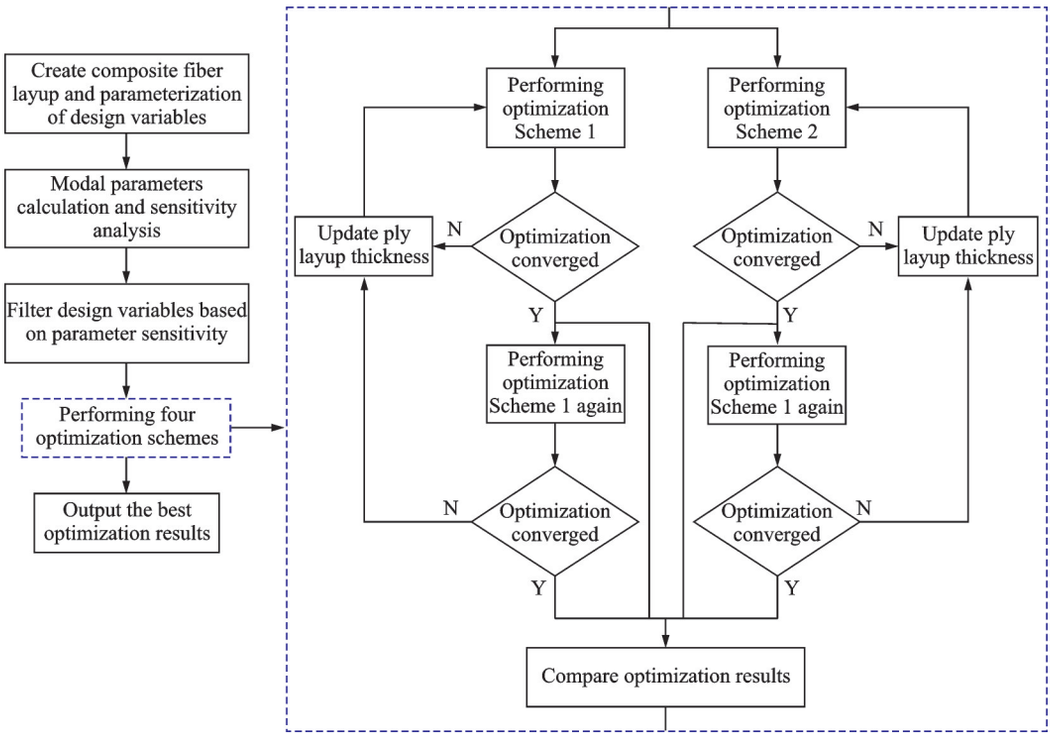

Fig.5 Flow chart of performing optimization

Scheme 1: Optimize blade flapwise and edgewise bending stiffness according to the optimal mathematical model shown in Eq.(6).

Scheme 2: Optimize blade flapwise and edgewise bending stiffness according to the optimal mathematical model shown in Eq.(7).

Scheme 3: Based on the results of scheme 1, scheme 1 is performed one more time.

Scheme 4: Based on the results of Scheme 2, Scheme 1 is performed one more time.

The precondition gradient-based solver in ANSYS is select as the optimizer to solve this optimization problem. To guarantee that the optimal solution converge on the global maximum in the design space, the genetic algorithm with a robust search capability is selected to determine it.

3 Results and Discussion

3.1 Effect of layup thickness of blade on its natural frequencies

The modal sensitivity of all design variables from the six parts of the blade, blade root and its transition, leading edge, leading panel, spar flange, trailing panel and trailing edge is calculated and plotted in Fig.6(a)—Fig.6(e). A positive modal sensitivity indicates a positive correlation between the layer thickness and the natural frequency, while a negative modal sensitivity means a negative correlation. The larger the absolute value of the modal sensitivity, the greater the influence of the parameters on the natural frequency of the blade. In the optimization of blade stiffness, parameters with relatively high sensitivity should be selected, while parameters with relatively low sensitivity should be discarded. According to the sensitivity calculation results in Fig.6, remove the design variables with the absolute value of modal sensitivity below 0.14 and select the 14 significant design variables.

Fig.6(a) depicts the modal sensitivity of design variables at the leading edge, blade root, and transition. The design variables of these parts have significant effects on the first-order flapwise natural frequency of the blade are N, P, $A1$, $A3$, $A14$, and

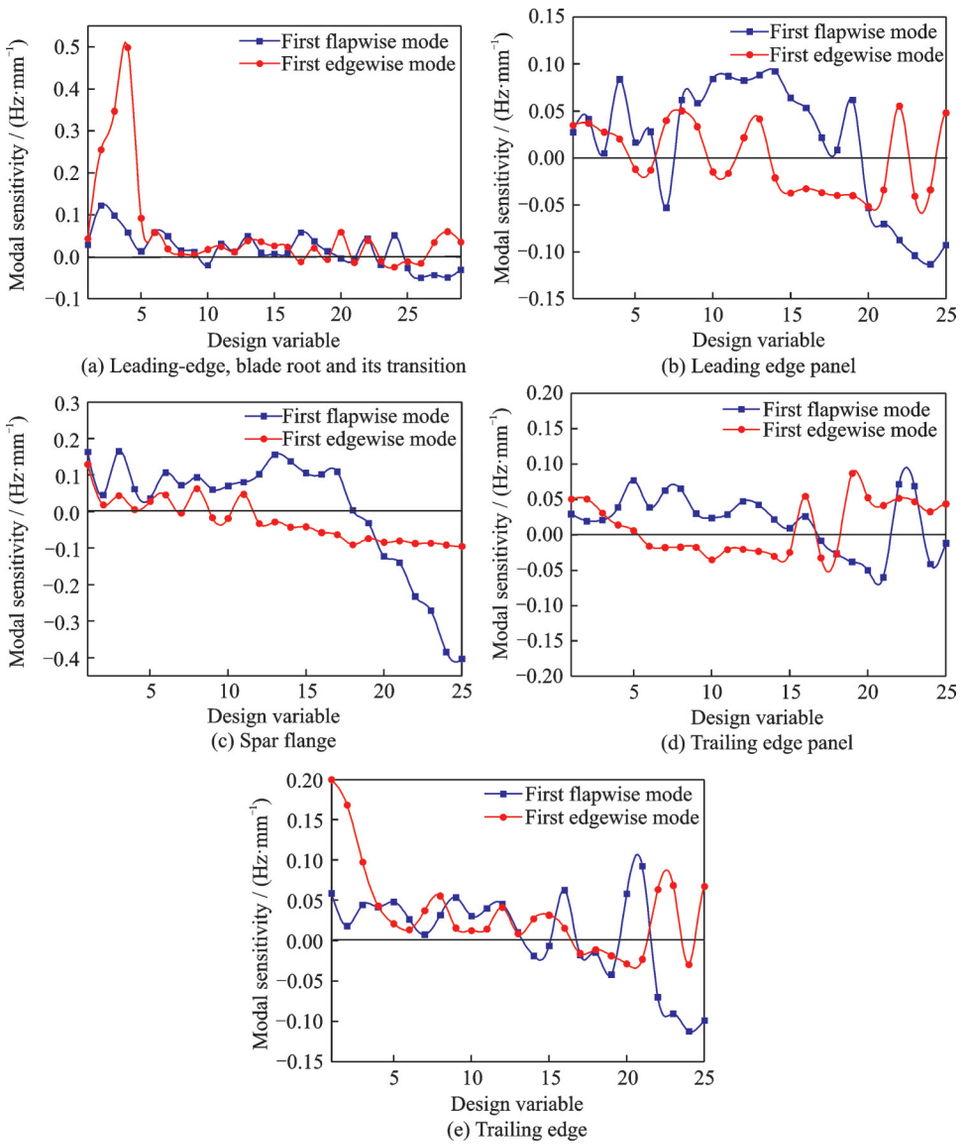

Fig.6 Modal sensitivity of design variables at each part of the blade

$A21$, the maximum sensitivity to the design variable N is 0.122 4 Hz/mm. These design variables influence the first-order edgewise natural frequency of the blade include N, P, $A1$ and $A2$. The maximum sensitivity to the design variable $A1$ of the first-order edgewise modes is 0.49 Hz/mm.

The modal sensitivity of layup thickness at the leading panel is marked in Fig.6(b). The design variables with relatively high first-order flapwise modal sensitivity in this position are $B4$, $B8$—$B16$, and $B19$, among which, the design variable $B4$ has the maximum sensitivity value of 0.092 Hz/mm. The effect of the design variables $B8$, $B22$ and $B25$ on the first-order edgewise natural frequency is relatively significant and $B22$ with the modal sensitivity value of 0.055 Hz/mm has the most conspicuous influence. Further analysis shows that all design variables at this part have a little effect on the natural frequency of the first-order flapwise and edgewise modes, and their modal sensitivity values are all less than 0.1 Hz/mm. This phenomenon occurs because the leading-edge panel is mainly subjected to shear loads and contributes trivially to flapwise and edgewise bending stiffness.

The modal sensitivity of layup thickness at the spar flange is shown in Fig.6(c). Since the spar flange mainly bears the flapwise load, the design variables at this position have a significant effect on the first-order flapwise natural frequency of the blade, but these design variables correspond to low

first-order edgewise modal sensitivity. The maximum absolute values of modal sensitivity for the first-order flapwise and edgewise mods are 0.4 Hz/mm and 0.13 Hz/mm, respectively.

Fig.6(d) illustrates the modal sensitivity of design variables at the trailing panel. The modal sensitivity of the design variables at the trailing panel has the same characteristic as the design variables at the leading panel, and both modal sensitivity values for the first-order flapwise and edgewise modes are all less than 0.1 Hz/mm. Therefore, the design variables of these two parts will be neglected in the subsequent structural optimization of the blade.

An illustration of the effect of the design variables at the trailing edge on the modal sensitivity of first-order flapwise and edgewise mode is shown in Fig.6(e). The trailing edge is a weak part of the blade, which basically does not bear the load. Therefore, the design variables at this part have a general trivial effect on the bending stiffness of the blade, but a few of these variables have a significant effect on the bending stiffness and cannot be ignored. For example, the design variables that have a non-negligible effect on the first-order flapwise natural frequency are $E1$, $E16$ and $E21$, and the design variables that have a significant impact on the first-order edgewise natural frequency are $E1$, $E2$, $E3$, $E8$, $E22$, $E23$ and $E25$.

3.2 Optimization results

3.2.1 Optimal results of the natural frequencies

The computed natural frequencies of first-order flapwise and edgewise modes of the blade and its weight from the four optimization schemes are displayed in Table 4.

It is evident from Table 4 that four optimization schemes all meet the weight constraints, and the natural frequencies from the four blades are increased by 7.5%—12% compared to the first blade. Further analysis showed that the optimization Scheme 3 increased the natural frequencies of the first-order flapwise and edgewise modes by up to 12% and 10.4% and obtained the best optimization results.

Table 4 Optimization results

Project	Mass/t	f_1/Hz	f_2/Hz
Initial blade	7.2	0.75	1.06
Scheme 1	7.2	0.82	1.14
Scheme 2	7.1	0.82	1.13
Scheme 3	7.2	0.84	1.17
Scheme 4	7.2	0.83	1.16

3.2.2 Optimal results of the layup thickness

The resulting curve of optimal layup thickness versus blade span for optimization Scheme 3 is plotted in Fig.7.

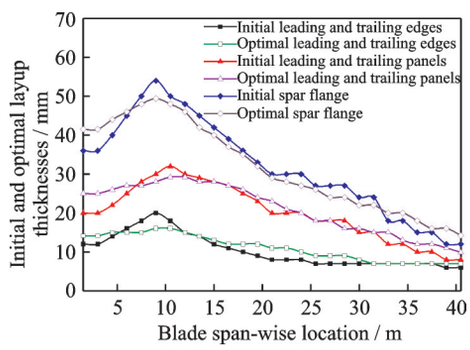

Fig.7 Comparison of layup thicknesses for initial and optimal blades.

Fig.7 shows that the initial parameters and optimal solutions are driving towards a similar trend, and the optimal solutions of optimization Scheme 3 vary greatly in maximum layup thickness for each part of the blade. For example, the optimal solution shows that the maximum layup thickness of the spar flange (4.6 mm reduction) compared to the initial blade, the leading and trailing panels (2.8 mm reduction), and the leading and trailing edges have a reduction of 4 mm. Another apparent trend is that the layer thickness of the areas near the blade root transition and the tip is increased to some extent after optimization, especially the layer thickness on the spar flange near the root transition with an increment of 5.5 mm. In general, the optimal solution shows that the thickness transition for any two adjacent areas is smoother than the initial's along the blade span.

The strength of the blade optimized in Scheme 3 is checked under extreme conditions, and the results show that its strength met the requirements. Therefore, the sensitivity analysis can provide the

modification direction for the dynamic modification of the blade structure, avoiding the blindness of the structural modification. Although manual modification can also improve the blade performance to a certain extent, only by using the optimized design based on the sensitivity analysis to realize the automatic optimization of the structure can we ensure the best blade performance, which ensures that the blade dynamic performance is optimized without increasing its weight.

4 Conclusions

This work develops a new selection approach on design variables from six parts of the blade in the structural design optimization of the wind turbine blades considering the flapwise and edgewise bending stiffness of the blade, and the selection of significant design variables based on the modal sensitivity analysis of layer parameters of the blade.

The analysis results show that the design variables that significantly affect the natural frequency of the first-order flapwise mode of the blade are basically distributed on the spar flange of the blade, and the modal sensitivity values of the design variables at this position are mostly higher than 0.1 Hz/mm. The design variables that have a significant effect on the natural frequency of the first-order edgewise mode are mainly located at the leading and trailing edges, especially the design variable $A1$ with a sensitivity value of 0.49 Hz/mm. Based on the modal sensitivity analysis of the layup thickness, a total of 14 design variables were selected to drive the structural optimization of the blade.

Four different strategies were explored to find an optimal distribution of composite layup thickness that improves the natural frequencies of a blade in both flapwise and edgewise directions. The third case increased the natural frequencies of the first-order flapwise and edgewise by 12% and 10.4%, respectively, achieving the desirable optimization results.

References

[1] PAVESE C, TIBALDI C, ZAHLE F, et al. Aeroelastic multidisciplinary design optimization of a swept wind turbine blade[J]. Wind Energy, 2017, 20(12): 1941-1953.

[2] AMANO R. Review of wind turbine research in 21st century[J]. Journal of Energy Resources Technology, 2017, 139(5): 050801.1-050801.8.

[3] LIU X, LU C, LIANG S, et al. Vibration-induced aerodynamic loads on large horizontal axis wind turbine blades[J]. Applied Energy, 2017, 185: 1109-1119.

[4] MISHNAEVSKY L, BRANNER K, PETERSEN H, et al. Materials for wind turbine blades: An overview[J]. Materials, 2017, 10(11): 1285.

[5] JENSEN J P, SKELTON K. Wind turbine blade recycling: Experiences, challenges and possibilities in a circular economy[J]. Renewable Sustainable Energy Reviews, 2018, 97: 165-176.

[6] JAVAID U, KHAN Z M, KHAN M, et al. Fabrication and thermo-mechanical characterization of glass fiber/vinyl ester wind turbine rotor blade[J]. Composites Part B Engineering, 2016, 91: 257-266.

[7] NETO J X V, JUNIOR E J G, MORENO S R, et al. Wind turbine blade geometry design based on multi-objective optimization using metaheuristics[J]. Energy, 2018, 162: 645-658.

[8] SHEN X, CHEN J G, ZHU X C, et al. Multi-objective optimization of wind turbine blades using lifting surface method[J]. Energy, 2015, 90: 1111-1121.

[9] DAXINI S D, PRAJAPATI J M. Parametric shape optimization techniques based on meshless methods: A review[J]. Structural and Multidiplinary Optimization, 2017, 56(5): 1197-1214.

[10] BARR S M, JAWORSKI J W. Optimization of tow-steered composite wind turbine blades for static aeroelastic performance[J]. Renewable Energy, 2019, 139: 859-872.

[11] ANDERSON E M, BHUIYAN F H, MAVRIPLIS D J, et al. Adjoint-based high-fidelity structural optimization of wind-turbine blade for load stress minimization[J]. AIAA Journal, 2019, 57(9): 4057-4070.

[12] ALMEIDA J H S, BITTRICH L, NOMURA T, et al. Cross-section optimization of topologically-optimized variable-axial anisotropic composite structures [J]. Composite Structures, 2019, 225: 111150.

[13] BUCKNEY N, GREEN S, PIRRERA A, et al. On the structural topology of wind turbine blades[J]. Wind Energy, 2013, 16(4): 545-560.

[14] CHEN J, WANG Q, SHEN W Z, et al. Structural

optimization study of composite wind turbine blade [J]. Mater Design, 2013, 46: 247-255.

[15] BOTTASSO C L, CAMPAGNOLO F, CROCE A, et al. Structural optimization of wind turbine rotor blades by multilevel sectional/multibody/3D-FEM analysis[J]. Multibody System Dynamics, 2014, 32(1): 87-116.

[16] SJOLUND J H, LUND E. Structural gradient based sizing optimization of wind turbine blades with fixed outer geometry[J]. Composite Structures, 2018, 203: 725-739.

[17] FAGAN E M, FLANAGAN M, LEEN S B, et al. Physical experimental static testing and structural design optimization for a composite wind turbine blade [J]. Composite Structures, 2017, 164: 90-103.

[18] ZHENG Y Q, ZHAO R Z. Characteristics for wind energy and wind turbines by considering vertical wind shear[J]. Journal of Central South University, 2015, 22(6): 2393-2398.

[19] MAHERI A. Multiobjective optimisation and integrated design of wind turbine blades using WTBM-ANSYS for high fidelity structural analysis[J]. Renew Energy, 2020, 145: 814-834.

[20] SUZUKI T, MAHFUZ H, TAKANASHI M. A new stiffness degradation model for fatigue life prediction of GFRPs under random loading[J]. International Journal of Fatigue, 2019, 119: 220-228.

Acknowledgements This work was supported by the National Natural Science Foundation of China (Nos. 51965034, 51565028) and the Lanzhou City Innovation and Entrepreneurship Project (No.2018-RC-25).

Authors Ms. **ZHENG Yuqiao** is an associate researcher in School of Electrical and Mechanical Engineering of Lanzhou University of Technology, Gansu Province, China. Her research interests include the dynamic characteristics and structural optimization.

Mr. **MA Huidong** received the B.E. degree from Lanzhou University of Technology, Lanzhou, China, in 2017. He is currently a postgraduate student at School of Mechanical and Electronical Engineering, Lanzhou University of Technology, Lanzhou, China. His research interests include structural optimization and reliability assessment of wind turbine blades.

Author contributions Ms. **ZHENG Yuqiao** provided valuable suggestions on the revision and improvement of the manuscript. Mr. **LIU Zheyan** contributed to the collection of experimental data. Mr. **MA Huidong** conducted the experimental analysis and wrote the manuscript. Mr. **ZHU Kai** contributed to the discussion and background of the study. All authors commented on the manuscript draft and approved the submission.

Competing interests The authors declare no competing interests.

(Production Editor: SUN Jing)

基于模态灵敏度的风力机复合材料叶片结构优化

郑玉巧，刘哲言，马辉东，朱 凯

（兰州理工大学机电工程学院，兰州 730050，中国）

摘要：提出了一种叶片全尺寸结构设计方法，该方法采用遗传算法确定叶片铺层厚度的最佳分布，从而使得叶片弯曲刚度最大化。采用数值微分法求解了叶片模态频率对叶片各子区域铺层厚度的灵敏度数值。选择了叶片一阶挥舞与摆振模态固有频率作为优化目标，基于模态灵敏度探究了各子区域铺层厚度对其挥舞与摆振刚度的影响，并筛选出了14个显著设计变量来驱动叶片结构优化。最优化结果显示叶片一阶挥舞与摆振频率分别提高了12%和10.4%，表明基于模态灵敏度的结构优化方法是一种提升叶片结构性能更为有效的方法。

关键词：复合材料叶片；离散化铺层厚度；模态灵敏度；最优厚度分布；弯曲刚度